Dissertation Abstract

Development of Triangular Microstrip Antenna for Sensor Application Using Circularly Polarized-Synthetic Aperture Radar

円偏波合成開口レーダを用いたセンサ応用のための正三角形マイクロストリップアンテナの開発

Graduate School of
Natural Science and Technology
Kanazawa University

Division of
Electrical Engineering and Computer Science

Student ID No.: 1624042014
Name: Muhammad Fauzan Edy Purnomo
Chief advisor: Prof. Akio Kitagawa
Date of submission: June 28, 2018

Abstract

Recently, many missions of Synthetic Aperture Radar (SAR) sensors are operated in linear polarization (HH, VV, and its combination) with high power, sensitive to Faraday rotation effect, etc. Newly, the development of radar technology, SAR and Unmanned Aerial Vehicle (UAV) are relatively fast which can generate data processed with high resolution and a better image for all types of terrain explored. The interest in the SAR system is expected to increase the research about the antenna which can be applied for developing SAR system.

Circularly Polarized-Synthetic Aperture Radar (CP-SAR) is as active sensor that could transmit and receive the *C*, *S*, and *L*-band chirp pulses for remote sensing application. The sensor is designed as a low cost, light, low power, low profile configuration to transmit and receive Left-Handed Circular Polarization (LHCP) and Right-Handed Circular Polarization (RHCP). Then, these circularly polarized waves are employed to generate the Axial Ratio Image (ARI), ellipticity and tilted angle images, etc. Hence, many information can be obtained from the earth and be able to overcome some limitations of the SAR sensor, such as high power, sensitive to Faraday rotation effect, the unwanted backscatter modulation signal and redistribution random back signal-energy, blurring and defocusing spatial variants, ambiguous identification, and low different features of backscatter.

In this research, we design triangular microstrip antennas both as basic construction and configuration of CP-SAR operated and embedded at the *S*-band and *L*-band on Low Earth Orbit (LEO) microsatellite and UAV having additional advantages such as a compact size, lightweight, conformability of the substrate surface, low cost, easier to integrate with other circuits, flexible, and well established. The investigation triangular microstrip antennas and its radiation characteristics are performed by numerical simulations and partly experiments aimed at CP-SAR sensor application.

The values of gain, axial ratio (*Ar*) and its bandwidth, azimuth and elevation beamwidth of gain and *Ar*, and antenna efficiency of triangular microstrip antennas are sufficient performances to meet the requirement of the specification of CP-SAR system using LEO microsatellite and UAV.

Keywords: CP-SAR, LHCP, RHCP, triangular microstrip antennas, LEO microsatellite, UAV

1. Introduction

The two main types of radar images are the circularly scanning Plan-Position Indicator (PPI) images and the side-looking images. The PPI applications are limited to monitor the air and naval traffic. The side-looking images applied in remote sensing are divided into two types: (i) Real Aperture Radar (RAR, usually called SLAR for Side-Looking Airborne Radar or SLR for Side-Looking Radar) (ii) Synthetic Aperture Radar (SAR).

The construction beam (Figure 1) tends to relatively tilted right toward UAV moving forward. Hence, one of many techniques to adjust beam direction is to excite the higher mode, especially the TM_{21}. When the antenna only has one element, the dominant mode is a role as the bigger beam rather than the higher mode of this patch [1]. But, when the antenna consist of array elements using corporate feeding-line (see parts 3.2 and 3.3), the antenna act as the higher mode (TM_{21}) CP that has the angle between the peak beam-direction and broadside around 20° until 50° depending on the values of dielectric constant of the substrate [2]. This condition happens because the location of corporate feeding-line is appropriately below the radiating patches having the perturbation segment.

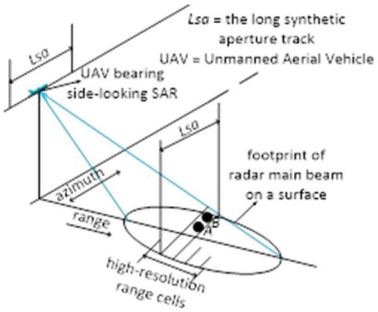

Figure 1. SAR configuration

In the Figure 1, the beam antenna is set to be perpendicular with the UAV path. Then, we can recognize that the range resolution is also perpendicular against the observation track and the azimuth resolution that will be parallel to the track. The range resolution for SAR is not different with common radar, and SAR technique gives no effect to this resolution. SAR only focus on making the azimuth resolution of a radar better than RAR.

In this research, the triangular microstrip antennas both as basic construction and configuration of CP-SAR application operated and embedded at the *S*-band and *L*-band on LEO microsatellite and UAV are investigated.

2. Approach of the research

In this research of microstrip antennas, the numerical simulation and partly to be confirmed with measurement in radio anechoic chamber are performed, then the results of them are discussed. One of the most common techniques for calculating the unknown current of the patch antenna is the Method of Moments (MoM). This method discretizes the integral into a matrix equation which can be solved. This discretization can be considered as dividing the antenna surface into a number of small elements. From the current distribution, the *S*-parameter, radiation pattern, and any other parameters of interest can be obtained. The software used is Ensemble^{TM} version 8 from Ansoft [3] for calculating the model of antennas: c1, c2, c3, c3s, and equilateral triangular, especially at the frequency around 2.5 GHz – 2.9 GHz as a basic construction of array antenna embedded on LEO (Low Earth Orbit) microsatellite for CP-SAR application. Among these models, the model of equilateral triangular antenna using dual feed type one is more appropriate to conduct a multi-polarization (LHCP = Left-Hand Circular Polarization and RHCP = Right-Hand Circular Polarization) array configuration. Because it is loaded with isolation parameter compared to probe feed. Then, we select the model of equilateral triangular with microstrip line dual feed type one to discuss rather than the model c1, c2, c3, and c3s. Also, we use the software of Computer Simulation Technology (CST) version 2016 from corporate company CST STUDIO SUITE [4] to simulate the triangular microstrip antenna at a resonant frequency, f = 1.25 GHz. It is lied on airspace and discussed two from three parts (a) LHCP and RHCP single patch antennas, (b) LHCP and RHCP modified lossless T-junction power divider 2 × 1, (c) LHCP and RHCP array two patches antennas using the modified lossless T-junction power divider 2 × 1, i.e., parts (b) and (c) as basic construction of array antenna embedded on UAV for CP-SAR application. Furthermore, the configuration of equilateral triangular array antennas designed with truncated-tip including radiating patches and corporate feeding-line with their parameters at the resonant frequency, f = 1.25 GHz are denoted and discussed one of three parts (i) LHCP and RHCP triangular array four patches antennas, (ii) LHCP and RHCP triangular array eight patches antennas, (iii) LHCP and RHCP triangular array sixteen patches antennas, i.e., part (iii) because if the targeted elevation beamwidth in range 3.57°– 31.02° at Table 1, only sixteen patches antenna for UAV can obtain it.

The parameter sizes of each patch are the same, namely the length of triangle side, a = 95.2311 mm and p = 101.38 mm, the length of perturbation segment, h = 7.64 mm and t = 1.5008 mm. The corporate feeding-line has two nodes (four patches), seven nodes (eight patches), fifteen nodes (sixteen patches) of T-junction having a function to distribute the current from the input port to output ports and to reach 2 × 2, 2 × 4, and 2 × 8 patches, respectively. The same length from input port to output ports are around 3.75λ or 610.5 mm (four patches), 5.25λ or 854.7 mm (eight patches), and 7.9λ or 1286.12 mm (sixteen patches). For a symmetric corporate feeding-line that the number of radiating patches is 2^m with some requirements. (i) m is an integer indicating the number of T-junctions toward patches for one patch, two and four patches. (ii) While for eight patches, m is an integer denoting the number of T-junctions which are not through patches. (iii) For sixteen, thirty-two, sixty-four, one hundred and twenty-eight, etc. patches, m is an integer exhibiting the number of T-junctions which are not through patches and input port divided by two and added with one.

To obtain the triangular array antenna operating TM_{21} CP, we use the following rules [5, 6]: (i) The truncated-tip radiating patches cooperated with corporate feeding-line have proper setting size, (ii) Right-angle bend and T-junctions connected with the corporate feeding-line have lossless transmission, (iii) The element spacing of adjacent radiating patches is around λ/2, (iv) In order to preserve the symmetric beam and to keep the low CP and the higher gain, the unwanted beams need to be suppressed.

One of the major steps in designing of microstrip patch antenna is to choose a suitable dielectric constant with appropriate thickness and loss tangent. A thicker substrate will increase the radiation power,

reduce conductor loss, and improve impedance bandwidth. A low value of the dielectric constant will increase the fringing field at the patch periphery. A high loss tangent rises dielectric loss and then reduces antenna efficiency. In this research, we choose the antenna substrate namely Nippon Pillar Packing (NPC) H220A which use a conventional substrate with dielectric constant or relative permittivity (ε_r) and loss tangent (δ) are 2.17 and 0.0005, respectively. Moreover, the substrate thickness of 1.6×2 (radiating patches and corporate feeding-line) is 3.2 mm. It is intended to attain the optimal performance of antenna characteristics that conform with a technical specification of CP-SAR system using the *L*-Band LEO microsatellite and UAV at Table 1 [7].

Table 1. Specification of antenna parameter for CP-SAR System

No	Parameter	Specification CP-SAR System
1.	Frequency (GHz)	*L*-band: 1.25-1.27 GHz; *S*-band: 2.5–2.9 GHz
2.	Pulse Band Wide (MHz)	10 - 233.31
3.	Axial Ratio (dB)	≤ 3
4.	Antenna Efficiency (%)	> 80
5.	Gain Antenna (dBic)	10 – 36.6
6.	Azimuth Beamwidth (°)	≥ 1.08 or 3.57 – 31.02
7.	Range Beamwidth (°)	≥ 2.16
8.	Antenna Size (m)	2 × 4
9.	Polarization (*Tx*/*Rx*)	LHCP + RHCP

3. Antennas configuration

3.1 Model equilateral triangular antenna

Figure 2 depicts the configuration of an optimized single equilateral triangular patch antenna with its fabrication and parameters. The patch antenna is fed by microstrip line to obtain a thin shape. The purpose of dual feed type one is to generate LHCP by using equilateral triangular patch antenna without truncated-tips, which one of the microstrip line feed is longer than the other to introduce a 90° phase delay. The antenna is made of a thin conducting patch that the radiating patch and microstrip line feed is located on the same layer which has a thickness, h = 1.6 mm and uses a conventional substrate (ε_r = 2.17 and δ = 0.0009) [8].

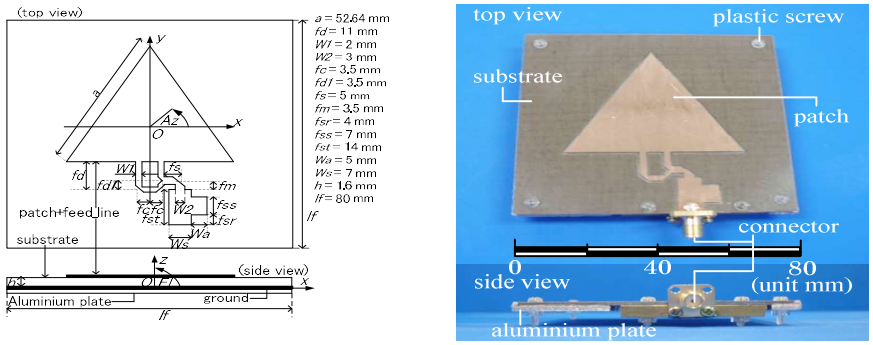

Figure 2. Configuration of equilateral triangular antenna

3.2 Model equilateral triangular truncated-tip antenna

3.2.1 LHCP and RHCP modified lossless T-junction power divider 2 × 1 configuration

The power divider is a network with one input port and *N* output ports. The input power at the input port would be divided by the number of the output ports that yield the same output power at each output port. One common characteristic found in power dividers is reciprocity. A reciprocal device is the one in which the transmitted power between two ports of device is the same regardless of the propagation direction through the device. For a reciprocal device [9-11], we have

$$[S] = [S]^T \; or \; S_{ij} = S_{ji} \; ; \; for \; all \; i \; and \; j \qquad (1)$$

Another property of the *S*-matrix is how much loss that can be attributed to the device. Ideally, a lossless power divider would be used in a system. However, the only low-loss divider is physically

realizable. It has been shown, particularly by Pozar, that if the *S*-matrix of the device is unitary, then the device is lossless, as follow [9-11]

$$[S]^T[S]^* = [I] \; or \; [S^*]^T[S] = [I] \tag{2}$$

Where [*I*] is the identity matrix, the superscript *T* represents the transpose of the matrix, and the superscript asterisk (*) represents the conjugate of the matrix.

By the definition, a -3 dB power divider is an ideal passive lossless reciprocal three ports device that divides power equally in magnitude and phase (see Figure 3). The *S*-parameter matrix related to this device is

$$[S] = \begin{bmatrix} S_{11} & S_{12} & S_{13} \\ S_{21} & S_{22} & S_{23} \\ S_{31} & S_{32} & S_{33} \end{bmatrix} \tag{3}$$

According to the matrix in (3), the condition for a lossless network is given by equation (2). Also, the condition for a reciprocal network is described in equation (1). Then, the condition for coefficient reflection load (Γ_L) is

$$\Gamma_L = 1 - \left|S_{ij}\right|^2 = \frac{reflection\ wave}{incident\ wave}; 0 \leq \Gamma_L \leq 1; i,j = 1,2,3 \tag{4}$$

If $\Gamma_L = 1\lfloor 0°$, then it occurs an open circuit condition. If $\Gamma_L = 1\lfloor 180°$, this is a short circuit condition. If $\Gamma_L = 0$, then this is a matched load circuit condition. Since, all the three ports of this power divider are matched, $S_{ii} = 0$. The modified *S*-matrix for matched load condition is

$$[S] = \begin{bmatrix} 0 & S_{12} & S_{13} \\ S_{21} & 0 & S_{23} \\ S_{31} & S_{32} & 0 \end{bmatrix} \tag{5}$$

In the *S*-matrix, the elements S_{23} and S_{32} are associated with the isolation between the output ports. These correspond to signals entering port 2 and exiting port 3, and vice versa. When the magnitudes of these elements are small, high isolation is achieved between the ports. For the lossless condition to be true, the matrix in equation (5) must be unitary and satisfy

$$|S_{12}|^2 + |S_{13}|^2 = 1 \tag{6}$$

$$|S_{12}|^2 + |S_{23}|^2 = 1 \tag{7}$$

$$|S_{13}|^2 + |S_{23}|^2 = 1 \tag{8}$$

$$S_{13}{}^* S_{23} = 0 \tag{9}$$

$$S_{23}{}^* S_{12} = 0 \tag{10}$$

$$S_{12}{}^* S_{13} = 0 \tag{11}$$

This condition means that two of the elements S_{12}, S_{13}, and S_{23} must be equal to zero to satisfy equations (9) – (10). For the sake of clarity of this analysis, S_{12} and S_{13} set equal to zero. However, it is clear that by setting S_{12} and S_{13} equal to zero, equation (6) is not satisfied. Consequently, when two of the elements S_{12}, S_{13}, and S_{23} are equal to zero, one of the equations (6) – (8) will not be satisfied. Thus a matched, reciprocal, lossless of three ports network becomes impossible to be realized [9-11].

3.2.2 Configuration of LHCP and RHCP array antennas using power divider 2 × 1

Figure 3 shows the configuration of triangular array antenna both LHCP and RHCP include the two radiating patches fed by corporate feeding-line with identical path lengths from the input port to output ports and their parameters. The equilateral triangular patch has a length, $a + t + h = p + 2t$ and a conventional substrate, $\varepsilon_r = 2.17$ and $\delta = 0.0005$. The parameter sizes of each patch (patch 1 and patch 2) are the same, namely the length of triangle side, $a = 95.2311$ mm and $p = 101.38$ mm, the length of perturbation segment, $h = 7.64$ mm and $t = 1.5008$ mm. Furthermore, the corporate feeding-line has one node of T-junction. This node has a function to distribute the current and to reach 2 × 1 patches having the same length from the input port to radiating patches or output ports around 9.32λ or 379.315 mm, where λ is wavelength.

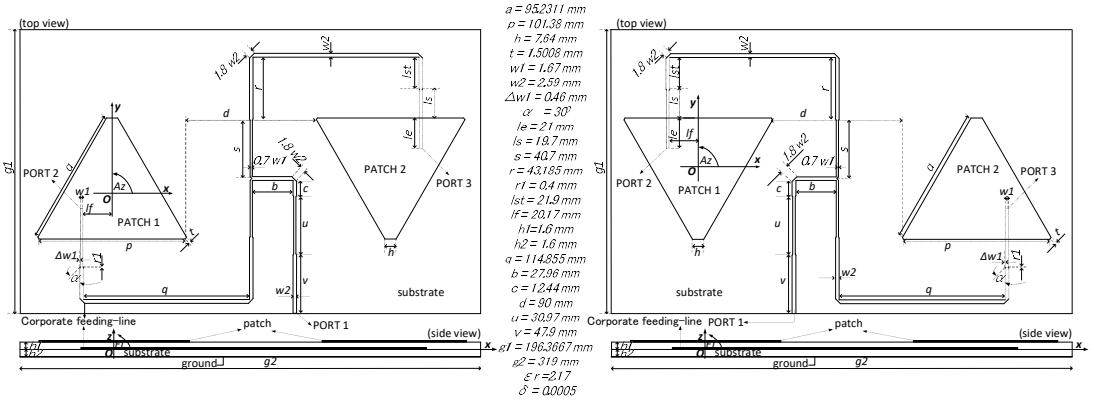

Figure 3. Configuration of LHCP and RHCP array antennas using power divider 2 × 1

3.3 Model LHCP and RHCP triangular array sixteen patches antennas

Figure 4 and Figure 5 show the configuration of triangular array antenna both LHCP and RHCP include the sixteen radiating elements/patches which are fed by 1:*n* (*n* is number of patches or *n* = 16) power divider network with identical path lengths from the input port to each patch or called corporate feeding-line, and their parameters [12, 13].

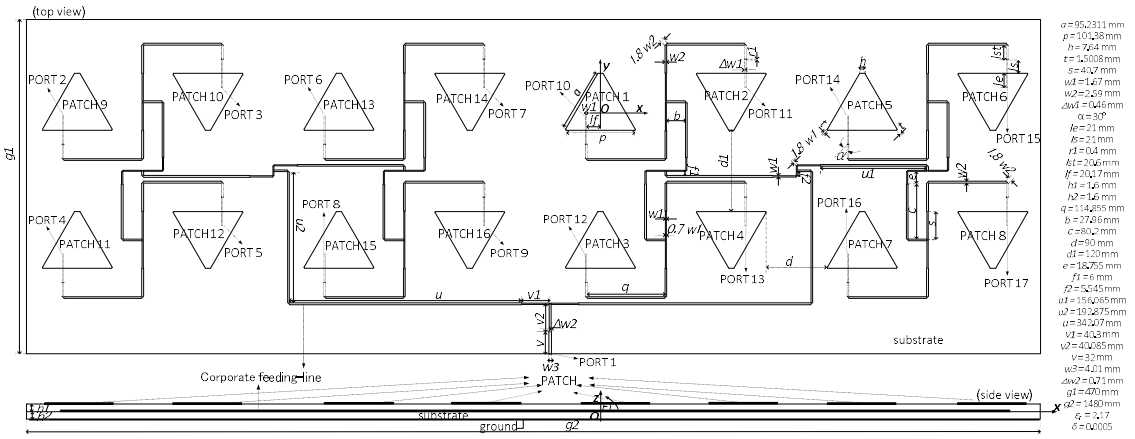

Figure 4. LHCP triangular array antenna 2 × 8 patches

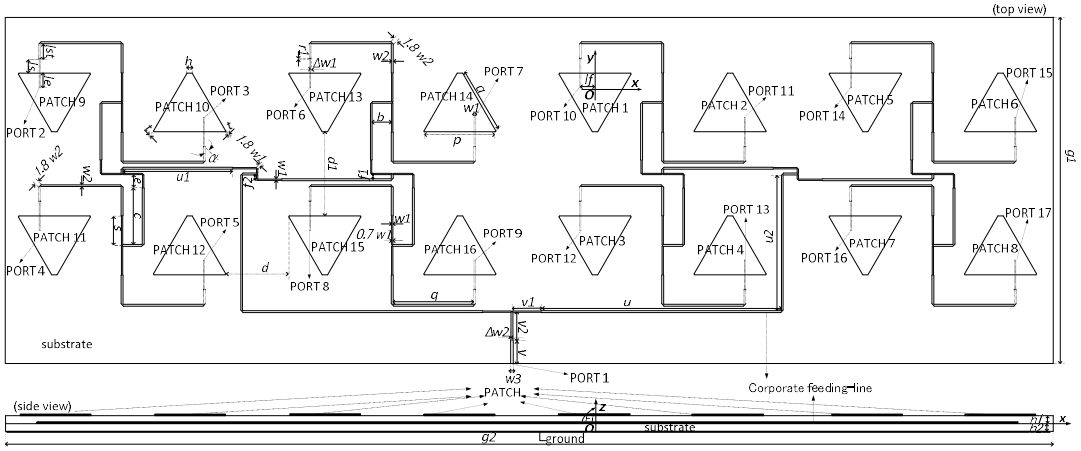

Figure 5. RHCP triangular array antenna 2 × 8 patches

4. Results and discussion

4.1 Model equilateral triangular antenna

Figure 6 shows the relationship between the reflection coefficient (*S*-parameter) and frequency for simulation and measurement of *Tx*/*Rx* antenna. From this figure, it can be seen that by comparison of the measurement with the simulation there is a frequency shifting about 1.5%.

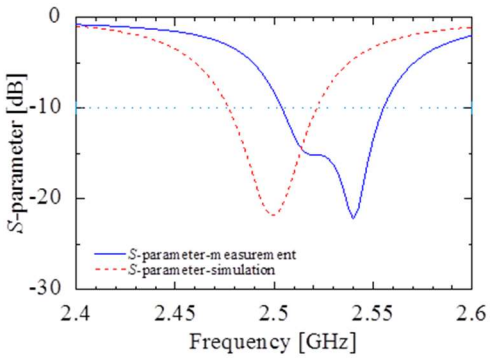

Figure 6. *S*-parameter

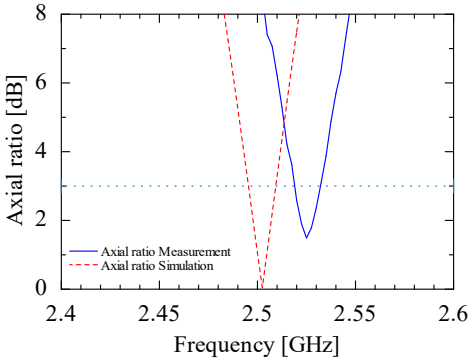

Figure 7. Axial ratio vs frequency

Figure 7 shows that the value of axial ratio (*Ar*) measurement increases of about 18% compared to the simulation (0.27 dB to 1.49 dB), also the frequency is shifted about 0.9% (2.5 GHz shifts to 2.53 GHz). Moreover, the bandwidth of axial ratio both simulation and measurement below 3 dB consecutive of about 0.02 GHz or 20 MHz and 0.015 GHz or 15 GHz meet for CP-SAR LEO microsatellite application.

Figure 8 and Figure 9 depict the relationship between gain-axial ratio vs elevation (*El*) and gain-axial ratio vs azimuth (*Az*) in the area of $El = 90°$ or $\theta = 0°$ at the resonant frequency, $f = 2.5$ GHz for simulation and $f = 2.53$ GHz for measurement. The 3-dB *Ar*-elevation beamwidth for simulation and measurement are successively about 120° and 80°. These values satisfy the targeted elevation beamwidth of ≥ 2.16° at Table 1. In addition, the values of the 3-dB *Ar*-azimuth beamwidth cover perfectly the whole of 360°. This result exhibit that the targeted azimuth beamwidth of ≥ 1.08° obtains the resolution of CP-SAR using LEO microsatellite.

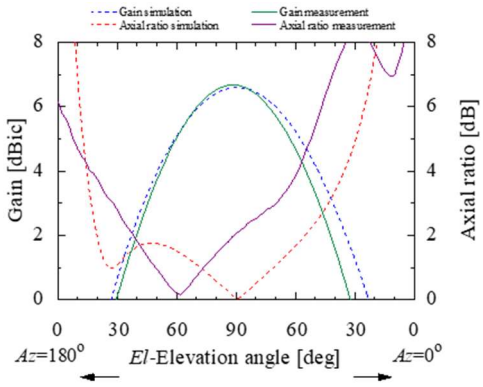

Figure 8. Elevation-cut plane

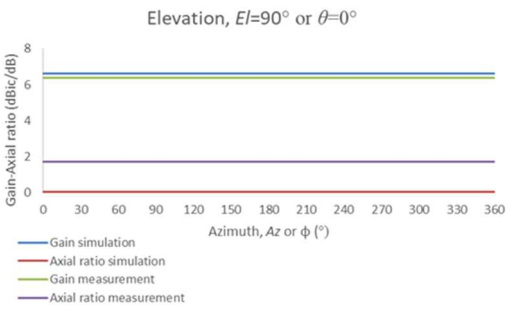

Figure 9. Azimuth-cut plane

4.2 Model equilateral triangular truncated-tip antenna

The real and imaginary parts of *S*-matrix both of LHCP and RHCP (Figure 3) of modified lossless T-junction power divider at $f = 1.25$ GHz taken from CST software are shown in equation (12) and (13), respectively.

$$[S]_{LHCP} = \begin{bmatrix} 0.04 + j0.16 & 0.44 - j0.53 & 0.43 - j0.54 \\ 0.44 - j0.53 & -0.39 - j0.08 & 0.55 + j0.09 \\ 0.43 - j0.54 & 0.55 + j0.09 & -0.38 - j0.07 \end{bmatrix} \quad (12)$$

We define that $[S]^T{}_{LHCP}$ and $[S]^*{}_{LHCP}$ are transpose and a conjugate matrix of (12), respectively.

$$[S]_{RHCP} = \begin{bmatrix} 0.04 + j0.16 & 0.43 - j0.54 & 0.44 - j0.53 \\ 0.43 - j0.54 & -0.38 - j0.07 & 0.55 + j0.09 \\ 0.44 - j0.53 & 0.55 + j0.09 & -0.39 - j0.08 \end{bmatrix} \quad (13)$$

Also, we notice that $[S]^T{}_{RHCP}$ and $[S]^*{}_{RHCP}$ are consecutively transpose and a conjugate matrix of (13). For reciprocity, they are clear for both LHCP and RHCP, i.e., $[S]_{LHCP} = [S]^T{}_{LHCP}$ and $[S]_{RHCP} = [S]^T{}_{RHCP}$. The matched ports of the divider set for LHCP S_{11} = 0.04 + j0.16, S_{22} = -0.39 - j0.08, and S_{33} = -0.38 - j0.07 and for RHCP S_{11} = 0.04 + j0.16, S_{22} = -0.38 - j0.07, and S_{33} = -0.39 - j0.08 are relatively close to zero. It means that only a little bit of the incident waves on the matched port will be reflected or not exit the ports. Thus, the reflected waves at the ports will close to zero. We get that both LHCP and RHCP are almost the lossless of the power divider, $[S]^T[S]^* = [I]$ *or* $[S^*]^T[S] = [I]$, as seen in (14) and (15).

$$[S]^T[S]^*{}_{LHCP} = \begin{bmatrix} 0.9782 & -0.0085 - j0.0022 & -0.0005 - j0.0054 \\ -0.0085 + j0.0022 & 0.9436 & 0.0384 + j0.0051 \\ -0.0005 + j0.0054 & 0.0384 - j0.0051 & 0.9364 \end{bmatrix} \approx \begin{bmatrix} 1 & 0 & 0 \\ 0 & 1 & 0 \\ 0 & 0 & 1 \end{bmatrix} \quad (14)$$

$$[S]^T[S]^*{}_{RHCP} = \begin{bmatrix} 0.9782 & -0.0005 - j0.0054 & -0.0085 - j0.0022 \\ -0.0005 + j0.0054 & 0.9364 & 0.0384 - j0.0051 \\ -0.0085 + j0.0022 & 0.0384 + j0.0051 & 0.9436 \end{bmatrix} \approx \begin{bmatrix} 1 & 0 & 0 \\ 0 & 1 & 0 \\ 0 & 0 & 1 \end{bmatrix} \quad (15)$$

Based on the design antenna using corporate feeding-line on Figure 3, the results are shown in Figure 10 until Figure 14. Figure 10 shows the relationship between the reflection coefficient (S_{11}) and the frequency for the simulation *Tx*/*Rx* triangular array antennas. Moreover, the S_{11} values at the resonant frequency for LHCP = -19.43 dB and for RHCP = -19.40 dB. Besides, the S_{11} bandwidth both LHCP and RHCP are similar around 37 MHz (2.96%). Figure 11 depicts that the values of gain and axial ratio for simulation of triangular array antennas in the direction of θ = -29° for LHCP and θ = 30° for RHCP at the resonant frequency, f = 1.25 GHz, are about 7.63 dBic, 2.68 dB, 7.62 dBic, and 2.74 dB, respectively.

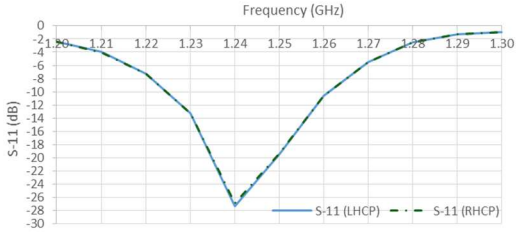

Figure 10. *S*-parameter 2 × 1 patches

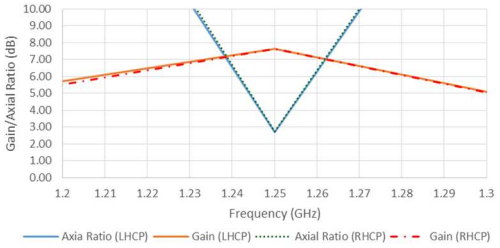

Figure 11. Frequency characteristic 2 × 1 patches

Figure 12 and Figure 13 depict the relationship between elevation-cut plane (θ = 0°) and azimuth-cut plane produced from the triangular array 2 × 1 antennas both LHCP and RHCP. The values of 3-dB *Ar*-elevation beamwidth for LHCP are 45° from -65° to -20° (*Az* = 180° or negative-θ) and 25° from 30° to 55° (*Az* = 0° or positive-θ). While for RHCP are 27° from -57° to -30° (*Az* = 180° or negative-θ) and 57° from 5° to 62° (*Az* = 0° or positive-θ). Moreover, the major values of 3-dB *Ar*-azimuth beamwidth of LHCP are about 57° from ϕ = 308° to ϕ = 5° and around 50° from ϕ = 130° to ϕ = 180°. While for RHCP are roughly 55° from ϕ = 0° to ϕ = 55° and approximately 45° from ϕ = 180° to ϕ = 225°. All of these values satisfy the targeted elevation beamwidth of ≥ 2.16° and the targeted azimuth beamwidth of ≥ 1.08° at Table 1.

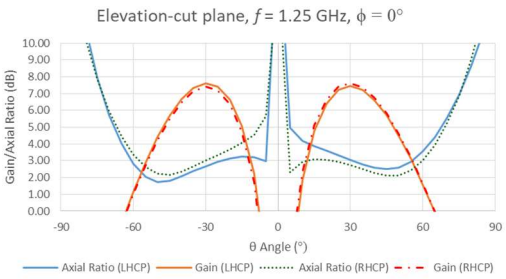

Figure 12. Elevation-cut plane 2 × 1 patches

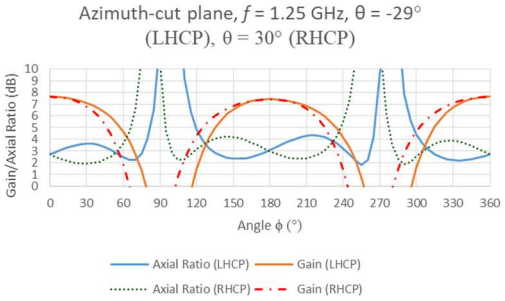

Figure 13. Azimuth-cut plane 2 × 1 patches

4.3 Model LHCP and RHCP triangular array sixteen patches antennas

However, when the radiating patches and the modified lossless T-junction power divider 2 × 8 network are run in the CST software, then the results show in Figure 14 to Figure 15 for simulation of triangular array antenna 2 × 8, in the case of *S*-parameter, frequency characteristic, radiation pattern, and antenna efficiency.

Figure 14 shows the S_{11} values at the resonant frequency for LHCP = -20.44 dB and for RHCP = -20 dB. Besides, the S_{11} bandwidth both LHCP and RHCP are similar around 34 MHz (2.72%). Figure 16 describes that the values of gain and axial ratio for simulation of triangular array antenna 2 × 8 at the direction of θ = 38° for LHCP and θ = -38° for RHCP at the resonant frequency, f = 1.25 GHz are about 16.55 dBic, 2.4 dB, 16.52 dBic, and 2.58 dB, respectively. Moreover, the 14 dBic gain-bandwidth and the 3-dB *Ar*-bandwidth both for LHCP and RHCP are the same around 54 MHz (4.32%) and 6 MHz (0.48%), respectively.

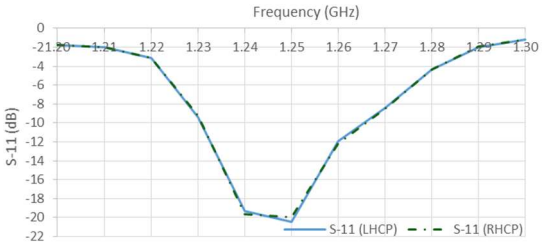

Figure 14. *S*-parameter 2 × 8 patches

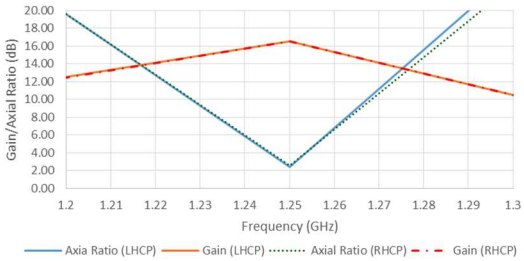

Figure 15. Frequency characteristic 2 × 8 patches

Figure 16 and Figure 17 depict the relationship between gain and elevation or θ-angle produced from the triangular array antenna both LHCP and RHCP (negative-θ for azimuth, Az = 180° or 270° and positive-θ for Az = 0° or 90°) as azimuth direction of CP-SAR at f = 1.25 GHz (see Figure 16 for Az = 0° or *x*-*z* plane and Figure 17 for Az = 90° or *y*-*z* plane). At the elevation -38° and 38° the average maximum gain and the average axial ratio values of the triangular array antennas are about 16.54 dBic and 2.49 dB in both of azimuth angle, respectively.

Figure 16 shows the beamwidth of the major lobes that exceed the target gain of 14 dBic both LHCP and RHCP around 10°, from -45° to -35° (Az = 180° or negative-θ) and from 35° to 45° (Az = 0° or positive-θ). Moreover, the simulated *Ar*-beamwidth of 3 dB for LHCP are 27° from -47° to -20° and 25° from 25° to 50°. While for RHCP are 12° from -47° to -35° and 33° from 17° to 50°. In Figure 17, similar curves are seen for the simulated results of Az = 90° and Az = 270°. The gain-beamwidth at 14 dBic both LHCP and RHCP are almost the same at around 10°, from -45° to -35° and from 35° to 45°. Furthermore, the simulated 3-dB *Ar*-beamwidth for LHCP approximate 27° from -47° to -20° (Az = 270° or negative-θ) and 25° from 25° to 50° (Az = 90° or positive-θ). While for RHCP are around 12° from -47° to -35° and about 33° from 17° to 50°. All of these values satisfy the targeted elevation beamwidth of 3.57° – 31.02° at Table 1 for better resolution of CP-SAR using UAV.

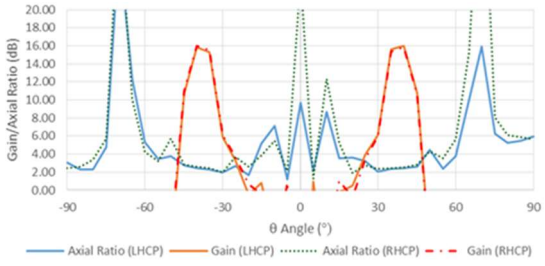

Figure 16. Elevation *x-z* plane, 2 × 8 patches

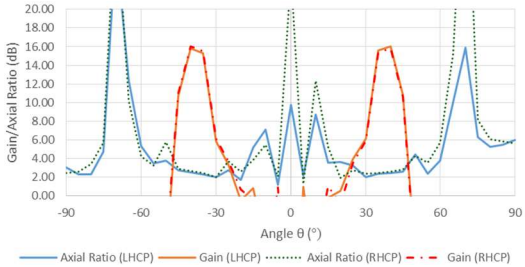

Figure 17. Elevation *y-z* plane, 2 × 8 patches

Figure 18 describes the characteristic of azimuth/conical pieces radiation generated by the triangular array antenna in the area of θ = 38° for LHCP and θ = -38° for RHCP at the resonant frequency of 1.25 GHz. From this figure, we can see that the peaks of the LHCP-gain and RHCP-gain are 16.55 dBic and 16.52 dBic at ϕ = 0° also 16.29 dBic and 16.36 dBic at ϕ = 180°, respectively. While the axial ratio values of LHCP and RHCP are consecutively 2.4 dB and 2.58 dB at ϕ = 0° likewise 2.42 dB and 2.519 dB at ϕ = 180°. In addition, the values of the gain-beamwidth of 14 dBic for LHCP are roughly 37° (from ϕ = 340° to ϕ = 17°) and approximately 35° (from ϕ = 165° to ϕ = 200°). When for RHCP are about 37° (from ϕ = 340° to ϕ = 17°) and some 30° (from ϕ = 155° to ϕ = 185°). Moreover, the values of the axial ratio beamwidth of 3 dB of LHCP are about 70° from ϕ = 325° to ϕ = 35° and from ϕ = 145° to ϕ = 215°. While for RHCP are roughly 75° from ϕ = 320° to ϕ = 35° and approximately 85° from ϕ = 130° to ϕ = 215°. These results exhibit that the targeted azimuth beamwidth of ≥ 6.77° obtains the resolution of CP-SAR using UAV. The antenna efficiency at resonant frequency of 1.25 GHz, for LHCP = 83.59% and for RHCP = 83.19% (see Figure 19). This result denotes that the antenna efficiency of 80% is acquired for CP-SAR using UAV.

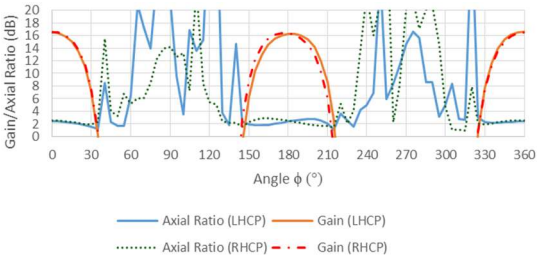

Figure 18. Azimuth *x-y* plane, 2 × 8 patches

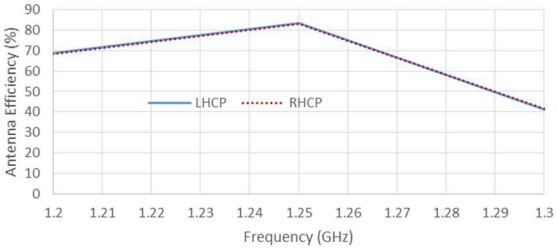

Figure 19. Antenna efficiency, 2 × 8 patches

5. Conclusions and future works

The conclusion for this research are as follow:

- The triangular shaped of patch antenna is chosen due to small size and practical for array antenna design in which the Transmitter (*Tx*) and Receiver (*Rx*) can be simultaneously arranged in a planar array compared with other shapes like the rectangular and circular patch antenna.
- To obtain a basic construction for CP-SAR geostationary satellite at *f* = 2.5 GHz – 2.9 GHz with compact, small, and simple configuration, the truncated-tip model c1, c2, c3, c3s, and microstrip line feed triangular antennas have been studied [8].
- While to acquire a basic construction for CP-SAR aircraft application at *f* = 1.25 GHz using proximity couple feed of single patch and array 2 × 1 patch antennas have been studied.
- The values of gain and axial ratio (*Ar*) for four patches antenna at the resonant frequency (*f* = 1.25 GHz) are 11.02 dBic and 2.47 dB (LHCP at θ = -30°) and 10.96 dBic and 2.45 dB (RHCP at θ = 31°), respectively [14].
- The values of gain and *Ar* for eight patches antenna at *f* = 1.25 GHz are 13.46 dBic and 1.89 dB (LHCP at θ = -36°) and 13.46 dBic and 1.9 dB (RHCP at θ = 36°), respectively [15].
- The values of gain and *Ar* for sixteen patches antenna at resonant frequency, *f* = 1.25 GHz are about 16.55 dBic and 2.4 dB (LHCP at θ = 38°), and around 16.52 dBic and 2.58 dB (RHCP at θ = -38°) [13].
- The targeted elevation beamwidth of ≥ 2.16 in Table 1 that all of the antenna both single and array antennas are satisfied the target, but if the targeted elevation beamwidth as reference, i.e., in range

3.57°– 31.02° at Table 1, only sixteen patches antenna for UAV can obtain it.

- The targeted azimuth beamwidth both of ≥ 1.08 and ≥ 6.77° (Table 1) for all antennas have been achieved using LEO microsatellite, aircraft, i.e., drone, small UAV, and UAV.
- Four, eight, and sixteen patches antennas both LHCP and RHCP can attain the targeted of 80% antenna efficiency at f = 1.25 GHz for CP-SAR using aircraft.

The continuity of the research in the next step are as follow:

- Develop the configuration of radiating patches antenna and corporate feeding-line based on proper theory of array antenna and network power divider to enhance the axial ratio bandwidth for two, four, eight, sixteen patches.
- Develop corporate feeding-line based on proper theory of power divider for array antenna of thirty-two, sixty-four, one hundred and twenty-eight, two hundred and fifty-six patches for CP-SAR aircraft and microsatellite applications.
- Design the Radio Frequency (RF) system and image/signal processing for CP-SAR application [16-17].
- The all of the antennas that are designed and discussed should be optimized, fabricated, measured, and done the outdoor experiment using CP-SAR sensor with aircraft and microsatellite [16-17].

References

[1] Baharuddin M., Wissan V., Sri Sumantyo J.T., Kuze H. *Equilateral microstrip antenna for circularly-polarized synthetic aperture radar*. Progress In Electromagnetics Research C., , 8, 107 – 120. 2009.

[2] Kishk A.A. and Shafai L. *The effect of various parameters of circular microstrip antennas on their radiation efficiency and the mode excitation*. IEEE Transactions on Antennas and Propagation, AP-34(8), 969 – 976. 1986.

[3] Ansoft Corporation. *ANSOFT Ensemble user guide manual (ver. 8)*. 2001.

[4] CST STUDIO SUITE 2016. *Microwave-radio frequency-optical*. Copyright © 1998–2016 CST AG. 2016.

[5] Horng T. S., Alexopoulos N. G. *Corporate feed design for microstrip arrays*. IEEE Transactions on Antennas and Propagation, Vol. 41, No. 12, 1615 – 1624. December 1993.

[6] Biao Du, Ning Yung E. K. *A Single-feed TM21 mode circular patch antenna with circular polarization*. Microwave and Optical Technology Letters, Vol. 33, 154 – 155. May 2002.

[7] Yohandri, et.al. *Development of circularly polarized array antenna for synthetic aperture radar sensor installed on UAV.* Progress In Electromagnetics Research C, Vol. 19, 119 – 133. 2011.

[8] Purnomo M. F. E. and Kitagawa A. *Analysis performance of triangle microstrip antenna for basic construction of circularly polarized-synthetic aperture radar application.* Jurnal TEKNOLOGI, Vol. 80, No. 2. March 2018. e-ISSN 2180-3722. DOI:https://doi.org/10.11113/jt.v80.11119.

[9] Pozar D. *Microwave Engineering*. John Wiley & Sons Inc. 3rd ed. Hoboken, New Jersey, 308 – 361. 2005.

[10] Grebennikov A. *RF and microwave transmitter design*. John Wiley & Sons Inc. Hoboken, New Jersey. 2011.

[11] Purnomo M. F. E. and Kitagawa A. *Triangular Microstrip Antenna for Circularly-Polarized Synthetic Aperture Radar Sensor Application*. Indonesian Journal of Electrical Engineering and Computer Science, Vol. 12, No. 1, October 2018. DOI:10.11591/ijeecs.v12.i1.pp310-318

[12] Gupta K.C., Garg R., Bahl I., Bhartia P. *Microstrip lines and slotlines*. Artech House, Inc. Second Edition. 1996. ISBN 0-89006-766-X.

[13] Purnomo M. F. E. and Kitagawa A. *Development of sixteen elements of microstrip triangular array antenna for circularly polarized-synthetic aperture radar sensor application*. J. Fundam. Appl. Sci., 10(5S), 535 – 550. 2018. DOI: http://dx.doi.org/10.4314/jfas.v10i5s.43

[14] Purnomo M. F. E. and Kitagawa A. *Developing basic configuration of triangle array antenna for circularly polarized-synthetic aperture radar sensor application.* Proceedings of IEEE 2017 International Conference on Radar, Antenna, Microwave, Electronics, and Telecommunications (ICRAMET 2017), 112 – 117. October 2017.

[15] Purnomo M. F E. and Kitagawa A. *Development of equilateral triangular array antenna with truncated-tip for circularly polarized-synthetic aperture radar sensor application*. Proceedings of 12th European Conference on Synthetic Aperture Radar, Session E.10. June 2018.

[16] Albert Aguasca, Rene Acevo-Herrera, Antoni Broquetas, Jordi J. Mallorqui, and Xavier Fabregas. ARBRES: Light-Weight CW/FM SAR Sensors for Small UAVs. Sensors 2013, 13, 3204 – 3216. 2013. ISSN 1424-8220. DOI:10.3390/s130303204.

[17] V. C. Koo, Y. K. Chan, V. Gobi, M. Y. Chua, C. H. Lim, C. S. Lim, C. C. Thum, T. S. Lim, Z. Ahmad, K. A. Mahmood, M. H. Shahid, C. Y. Ang, W. Q. Tan, P. N. Tan, K. S. Yee, W. G. Cheaw, H. S. Boey, A. L. Choo, and B. C. Sew. *A new unmanned aerial vehicle synthetic aperture radar for environmental monitoring*. Progress In Electromagnetics Research, Vol. 122, 245 – 268. 2012.

平成３０年　８月　９日

学位論文審査報告書（甲）

１．学位論文題目（外国語の場合は和訳を付けること。）

Development of Triangular Microstrip Antenna for Sensor Application Using Circularly Polarized-Synthetic Aperture Radar（円偏波合成開口レーダを用いたセンサ応用のための正三角形マイクロストリップアンテナの開発）

２．論文提出者　(1) 所　　属　電子情報科学　専攻

(2) 氏（ふり）　名（がな）　Muhammad Fauzan Edy Purnomo（むはまど ふあうざん えでぃ ぷるのも）

３．審査結果の要旨（600～650 字）

平成 30 年 8 月 9 日に第 1 回学位論文審査委員会を開催した。同日に口頭発表を実施し、その後に第 2 回審査委員会を開催した。慎重審議の結果、以下の通り判定した。なお、口頭発表に対する質疑を最終試験に代えるものとした。

合成開口レーダは、航空機や人工衛星に搭載され、海洋研究、気象観測、地学、防災、農業などの分野で広く利用されている。特に近年、無人航空機に搭載して、高解像度の地質や地形の画像を得るための小型のレーダ用アンテナが必要とされている。

本論文は、正三角形円偏波マイクロストリップアンテナの設計法および同アンテナを用いた高密度アレイアンテナの設計法を提案している。多数のアンテナをアレイ化することにより、レーダを高性能化することができる。正三角形円偏波マイクロストリップアンテナは、高密度に配置できるため、合成開口レーダ用アレイアンテナの小型化に有効であることが、理論、シミュレーション、実測データにより示された。

以上の研究により、小型の合成開口レーダ用アンテナの設計法が確立された。また、本研究の成果は、地震、豪雨、火山活動などの自然災害の状況の正確な判読および防災に貢献する。従って、本論文は博士（工学）に値すると判定した。

４．審査結果　(1) 判　　定（いずれかに○印）　○　合　格　・　不合格

(2) 授与学位　　博　士（工学）